FINITE ELEMENT ANALYSIS OF AXISYMMETRIC GEOMETRIES IN QUANTITATIVE NDE

R. Palanisamy and W. Lord
Department of Electrical Engineering
Colorado State University
Fort Collins, Colorado 80523

ABSTRACT

Solution of the inversion problem in quantitative eddy current NDE requires an adequate mathematical model to describe the complicated interactions of currents, fields and flaws in materials. Existing analytical techniques are not capable of accommodating materials with nonlinear magnetic characteristics or awkward flaw shapes.

This paper describes a finite element computation of the complex impedance of an eddy current sensor in axisymmetric testing configurations, some with defects and gives the corresponding magnetic flux distributions. The authors suggest that, because finite element analysis techniques are not limited by material nonlinearities and complex defect geometries, they can be applied to the development of computer based defect characterization schemes for realistic eddy current NDE applications.

INTRODUCTION

Nondestructive testing and evaluation play an important role in the design, fabrication and day-to-day maintenance of military, aerospace, electric power and transportation industry equipment. The economic impact of component failure in these industries is well documented[1-4] and, together with the obvious human and environmental implications, provides a major impetus to improve all aspects of the nondestructive testing art. Progress has been made toward this end through such efforts as the DARPA/AFML program[5]. Although the work has concentrated primarily on ultrasonic techniques, much of the research philosophy developed for the program with regard to the study of basic phenomena[6], development of models[7], signature identification by signal processing[8] and the subsequent accept/reject decision founded on a knowledge of fracture mechanics and related failure probabilities could and should be applied to other nondestructive testing techniques. The cornerstone of such an approach is the development of an adequate mathematical model for the study of basic field/defect interactions. Such a model is needed in order to develop a defect characterization scheme and to identify suitable parameters for signal processing.

In eddy current methods of nondestructive testing, alternating current excitation is used to induce secondary currents and fields in the specimen undergoing inspection. Defects in the specimen cause changes in both induced current and fields, resulting in measurable impedance variations in a nearby search coil. Despite recent developments in automatic defect characterization associated with eddy current and leakage flux methods of nondestructive testing[9-11], the subject of electromagnetic methods of nondestructively testing ferromagnetic materials is characterized largely by empirical knowledge. Where closed form mathematical solutions do exist, describing electromagnetic field/defect interactions, the underlying assumptions of the theories tend to invalidate any realistic application of the results to the problem of defect characterization.

The problem of modeling electromagnetic field/defect interactions in materials is complicated by any nonlinear magnetization characteristic of the material and awkward defect boundaries. For this reason, much of the existing literature associated with eddy current phenomena is concerned with making simplifying assumptions so that, for a given eddy current situation, closed-form expressions can be obtained for the normalized impedance of the search coil. Scott[12] gives an overview of the numerous mathematical approaches which lead to closed-form solutions of eddy current problems and references 13 through 26 describe these various classical approaches in more detail. Despite the apparent plethora of analysis techniques including wave theory, integral, network and finite difference formulations, the basic problem of developing a defect characterization scheme for realistic defects in nonlinear ferromagnetic materials still remains.

An approach which does show promise of providing the basis of defect characterization schemes for all electromagnetic NDT methods (active, residual and eddy current forms)[27] is the finite element analysis technique which was originally developed for the study of magnetic fields in electrical machinery[28-30]. Lord and Hwang have subsequently applied this technique[31-33] to the development of a defect characterization scheme for active leakage field methods of nondestructive testing. More recently, and again, building on work relating to electromagnetic machinery[34-42], it has been shown that eddy current NDT problems are tractable using the finite element approach[43-44]

The major purposes of this paper are to give a tutorial overview of the method and to extend the initial studies to an important class of eddy current NDT situations, namely those having axial symmetry.

THEORETICAL CONSIDERATIONS

The Diffusion Equation and Energy Functional - Consider a simply connected region R, the cross-section of an axisymmetric geometry, bounded by the curve C

in the r,z plane as shown in Fig. 1.

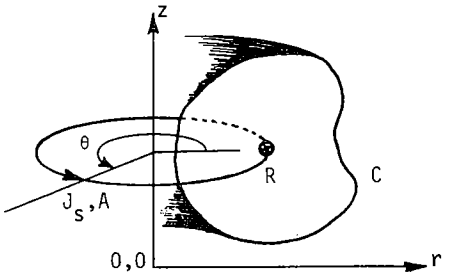

Fig. 1. Axisymmetric Geometry Showing the Direction of J_s and A.

The sinusoidal source current density J_s(amps/m^2) and hence the complex magnetic vector potential A (Webers/m) have components only along the positive θ direction. That is, both J_s and A are a function of r and z only. This situation can be modeled by a Poisson type of nonlinear diffusion equation[37]

$$\frac{\partial^2 A}{\partial r^2} + \frac{1}{r}\frac{\partial A}{\partial r} + \frac{\partial^2 A}{\partial z^2} - \frac{A}{r^2} = -\mu J_s + j\omega\sigma\mu A \qquad (1)$$

where μ = nonlinear magnetic permeability (Henry/m)

ω = angular frequency (rad/sec)

σ = electrical conductivity (mhos/m)

$j = \sqrt{-1}$, complex operator.

The eddy current density J_e(amps/m^2) is given by

$$J_e = -j\omega\sigma A \qquad (2)$$

From the principles of variational calculus, it can be shown that a correct solution of Eq. 1 can be obtained by minimizing the nonlinear energy functional

$$F = \iiint_V \left[\int \frac{1}{\mu} BdB + \frac{1}{2} j\omega\sigma|A|^2 - J_s \cdot A\right]dv \qquad (3)$$

where B = flux density (Webers/m^2), over the entire region of interest.

Finite Element Formulation - The very basis of finite element analysis is to search for a function A such that the energy functional F of Eq. 3 is minimized, instead of solving Eq. 1 directly.

The region R of Fig. 1 which contains the area of interest (including current sources, ferromagnetic material, etc.) must be of finite size if Eq. 3 is to be solved numerically. The boundary of the region is chosen such that the magnetic vector potential A is either zero along the boundary or the gradient of A is negligibly small along the boundary compared to the value elsewhere in the region. Discretization of this region is achieved as follows (see Fig. 2)[34]:

The chosen solution region (finite element region) is subdivided into triangles. The number, shape and size of these triangles are not restricted in any way.

- Interfaces between different materials must be formed by the sides of the triangles.
- In order to ensure a reasonable accuracy of the numerical solution, the triangles must be smaller in a region where the gradient of the magnetic flux density is larger.
- All the elements have the same unit depth of one radian in the θ direction.
- The current density, permeability and flux density are assumed to be constant within each triangular element.
- Along the boundary C, the magnetic vector potential is zero.

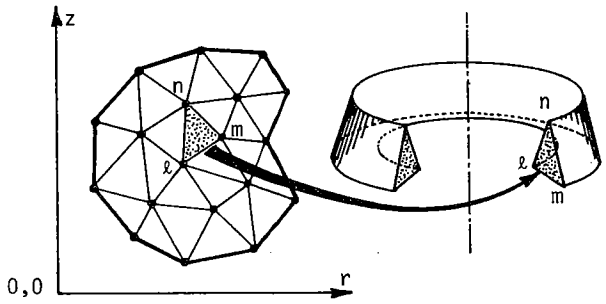

Fig. 2. Discretization of the Finite Element Region R, and a Typical Axisymmetric Finite Element ℓmn.

In order to set up the local element matrix equation the variation of function A within each element is assumed to be linear and dependent only on the values of A at the vertices. For example, the value of $A_p(r,z)$ at the point P(r,z) within the element ℓmn in Fig. 3 is given by

$$A_p(r,z) = \frac{1}{2\Delta} \sum_{i=\ell,m,n} (a_i + b_i r + c_i z)A_i \quad , \qquad (4)$$

where

$$a_\ell = r_m z_n - z_m r_n \qquad (5)$$

$$b_\ell = z_m - z_n \qquad (6)$$

$$c_\ell = r_m - r_n \qquad (7)$$

Δ is the area of the element ℓmn, and A_ℓ, A_m and A_m are the values of A at the vertices ℓ, m and n. Extending this approximation to all the elements in the region R, we obtain an approximate representation for A throughout the region. All the vertex (nodal) values of A in the region are varied simultaneously until the energy functional F given in Eq. 3 reaches a minimum, resulting in the final solution for A at all the nodes in the region.

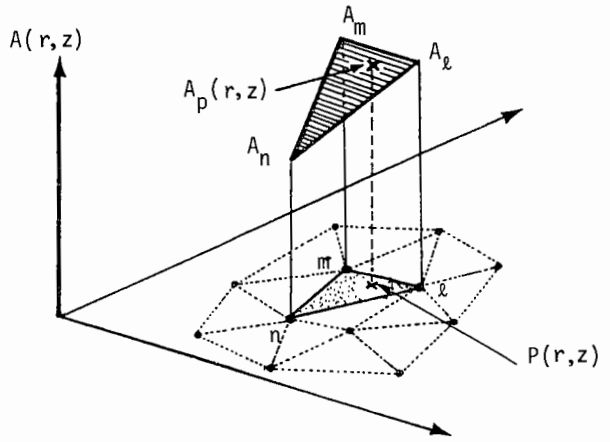

Fig. 3. Linear Approximation of Function A within a Triangular Finite Element, ℓmn.

Minimization of the energy functional F is achieved by setting the first derivative of F with respect to every vertex value equal to zero. That is

$$\frac{\partial F}{\partial A_k} = 0 \quad , \quad k=1,2,\ldots N \tag{8}$$

where N = total number of nodes in the region. Instead of performing the minimization node by node in sequence, for convenience, we perform it element by element. Substituting $A_p(r,z)$ from Eq. 4 in Eq. 3 and performing the following three operations simultaneously, i.e.

$$\frac{\partial F}{\partial A_i} = 0 \quad , \quad i=\ell,m,n \tag{9}$$

we obtain three equations in three unknown vector potential values (A_ℓ, A_m and A_n) for the element ℓmn.

After some algebra these equations are represented in the final matrix form as[37]

$$[[S]_e + j[R]_e]\{A\}_e = \{Q\}_e \tag{10}$$

where $[S]_e$ is a 3 x 3 'element matrix' formed from the r and z values of the three vertices ℓ, m and n and the area Δ in an element ℓmn, μ value associated with the element ℓmn, and the centroid of the element r_c from the z axis,

$$= \frac{r_c}{4\Delta\mu} \begin{bmatrix} (b'_\ell b'_\ell + c_\ell c_\ell) & (b'_\ell b'_m + c_\ell c_m) & (b'_\ell b'_n + c_\ell c_n) \\ (b'_m b'_\ell + c_m c_\ell) & (b'_m b'_m + c_m c_m) & (b'_m b'_n + c_m c_n) \\ (b'_n b'_\ell + c_n c_\ell) & (b'_n b'_m + c_n c_m) & (b'_n b'_n + c_n c_n) \end{bmatrix}$$

$$b'_k = b_k + \frac{2\Delta}{3r_c} \quad , \quad k = \ell,m,n$$

$[R]_e$ is a 3 x 3 'element matrix' formed from the angular frequency ω, electrical conductivity σ associated with the element ℓmn and the centroid r_c and area Δ of the element ℓmn,

$$= \frac{\omega\sigma\Delta r_c}{12} \begin{bmatrix} 2 & 1 & 1 \\ 1 & 2 & 1 \\ 1 & 1 & 2 \end{bmatrix}$$

$\{Q\}_e$ is a 3 x 1 'element_matrix' formed from the complex current density J_s within an element ℓmn,

$$= \frac{J_s\Delta r_c}{3} \begin{Bmatrix} 1 \\ 1 \\ 1 \end{Bmatrix}$$

$\{A\}_e$ is a 3 x 1 'element matrix' formed from the unknown complex vector potentials A_ℓ, A_m and A_n of an element ℓmn,

$$= \begin{Bmatrix} A_\ell \\ A_m \\ A_n \end{Bmatrix}$$

This is the finite element representation of the energy functional of Eq. 3 for a typical triangle ℓmn, in the region R. This approach now has to be extended to cover all the elements of region R to form the global matrix equation.

Element matrix equations corresponding to Eq. 10 can be formed separately for all the elements in the finite element region. These individual element equations are then combined into a single 'global matrix' equation

$$[G]\{A\} = \{Q\} \tag{11}$$

where [G] is a (NxN) banded symmetric complex matrix, and {Q} and {A} are (Nx1) complex column matrices. The expanded form of equation 11 is

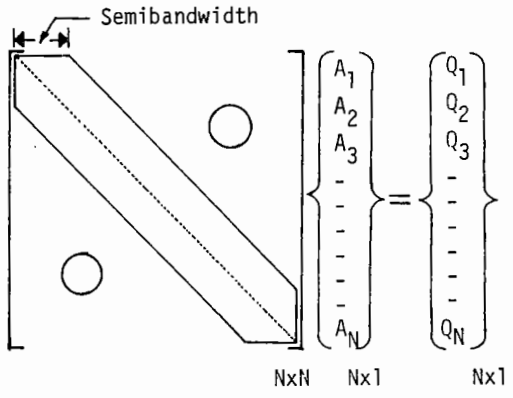

(12)

Any of the direct solution techniques (e.g. Gaussian elimination[45]) utilizing the banded symmetry and sparse nature of the global matrix, [G], can be applied to solve for the unknown vector potentials, A. Because of symmetry, it is sufficient to store only the elements in the semibandwidth of the matrix [G], and this brings down the computer storage requirement considerably.

Calculation of Flux Density - The relationship between the magnetic flux density B and the magnetic vector potential A is

$$B = \nabla \times A \tag{13}$$

Remembering that A has a component only along the positive θ direction, we obtain

$$B_r = -\frac{\partial A}{\partial z} \tag{14}$$

$$B_z = \frac{A}{r} + \frac{\partial A}{\partial r} \tag{15}$$

$$B_\theta = 0 \tag{16}$$

Within each finite element a linear variation of A is assumed[30].

$$A = \alpha_1 + \alpha_2 r + \alpha_3 z \tag{17}$$

Therefore,

$$B_r = -\alpha_3 \tag{18}$$

$$B_z = \frac{A}{r} + \alpha_2 \tag{19}$$

Taking A_c as the value of A at the centroid r_c (Fig. 4) of a triangular element, without loss of accuracy, we obtain

$$B_z = \frac{A_c}{r_c} + \alpha_2 \tag{20}$$

$$r_c = \frac{1}{3}(r_\ell + r_m + r_n)$$

$$A_c = \frac{1}{3}(A_\ell + A_m + A_n)$$

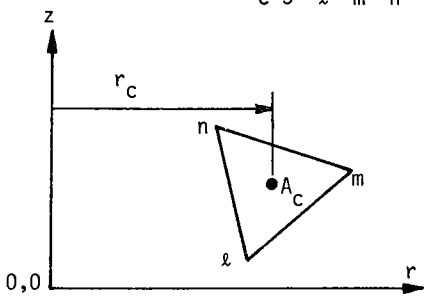

Fig. 4. Approximate values of r_c and A_c in an Element ℓmn.

The expressions for α_2 and α_3 can be obtained by simultaneously solving the three equations written for A_ℓ, A_m and A_n using Eq. 17. A_c and r_c can be calculated either as indicated in Fig. 4, or by using area coordinates for better accuracy[46]. That is,

$$r_c = \left[\frac{1}{12}\{r_\ell^2 + r_m^2 + r_n^2 + (r_\ell + r_m + r_n)^2\}\right]^{1/2} \tag{21}$$

and

$$A_c = \left[\frac{1}{12}\{A_\ell^2 + A_m^2 + A_n^2 + (A_\ell + A_m + A_n)^2\}\right]^{1/2} \tag{22}$$

Hence the final expression for the flux densities are

$$B_r = -\frac{1}{2\Delta}[A_\ell(r_n - r_m) + A_m(r_\ell - r_n) + A_n(r_m - r_\ell)] \tag{23}$$

$$B_z = \frac{A_c}{r_c} + \frac{1}{2\Delta}[A_\ell(z_m - z_n) + A_m(z_n - z_\ell) + A_n(z_\ell - z_m)] \tag{24}$$

Resultant flux density

$$B = (B_r^2 + B_z^2)^{1/2} \tag{25}$$

The simplified flow chart of Fig. 5 outlines the computational steps involved in the finite element analysis of eddy current problems.

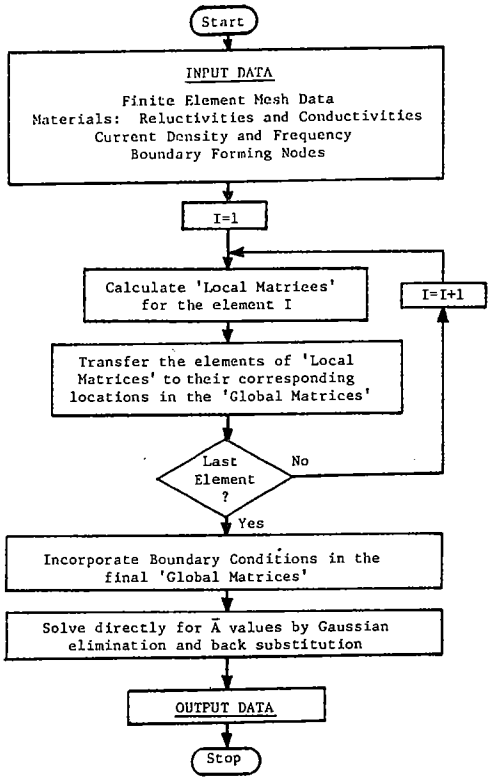

Fig. 5. Simplified Flow Chart for the Finite Element Analysis of Eddy Current Problems.

Normalized Complex Impedance (Z_n) of a Coil - The complex impedance of a circular coil can be calculated from the complex magnetic vector potential values. That is

$$Z = -\frac{j\omega 2\pi N}{I_s} \sum r_c A_c \Delta \tag{26}$$

where N is the turn density (turns/m^2) in the coil, I_s is the source current (amps), r_c is the centroidal distance os a triangular element from the z axis (meters), A_c is the complex magnetic vector potential

at the centroid of an element, and the summation is taken over all the elements forming the coil cross-section in the finite element region.

The normalized impedance, Z_n, useful for the complex impedance plane plot, is obtained by dividing Z with the reactance of the coil, ωL_o, where L_o is the self inductance of the coil in air. That is,

$$Z_n = \frac{Z}{\omega L_o} \qquad (27)$$

RESULTS

Initial emphasis in this work was placed on studying those eddy current geometries for which analytical solutions existed. Reference 44 describes the application of finite element analysis techniques to the problem of predicting the current density in a metal slab lying under a conductor carrying an alternating current. As the results agreed well with the analytical predictions of Stoll[14] the finite element studies were then extended to the axisymmetric geometries described in this paper. For the first three cases results are compared with those predicted by an ORNL program[26] based on integral equation concepts. Values of conductivity chosen for the aluminum copper and iron used in these studies were 28.6×10^6, 57.7×10^6 and 10×10^6 mhos/m respectively. Relative permeability values were 1.0 for aluminum and copper, and 100 for iron.

Case 1: - coil in air. Figures 6a), b) and c) show the geometry, finite element mesh and predicted flux distribution. The corresponding inductance values obtained using finite element (FE) and ORNL code are given in Table 1.

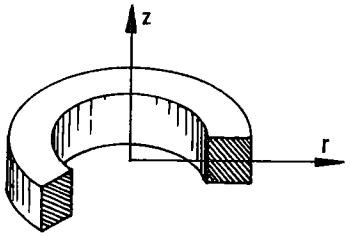

a)

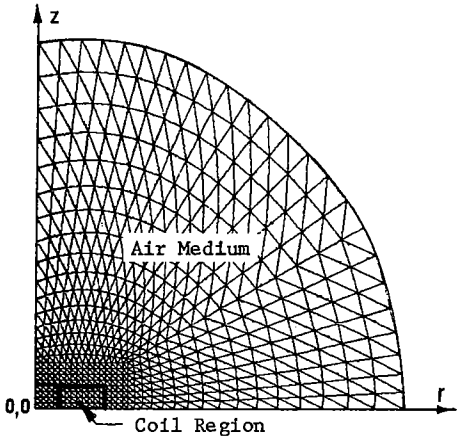

b)

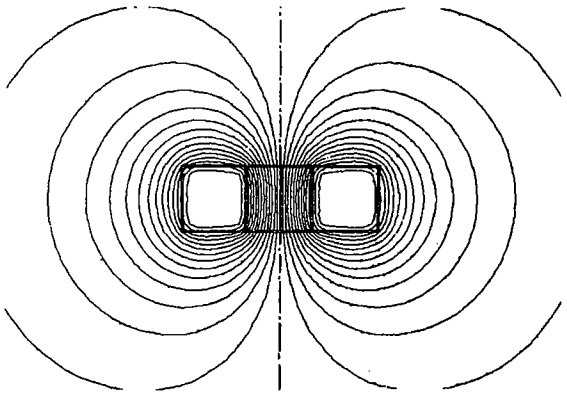

c)

Fig. 6. Circular eddy current coil: a) geometry, b) finite element mesh, c) predicted flux distribution.

Case	FE Code	ORNL Code
1. (Fig. 6). Self Inductance	3.216×10^{-4}H	3.217×10^{-4}H
2. (Fig. 7). Normalized Impedance	0.101 + j0.723	0.101 + j0.737
3. (Fig. 8). Normalized Impedance	0.109 + j0.649	0.108 + j0.647

Table 1. Estimated inductance values for cases 1, 2 and 3.

Case 2: - coil on a copper slab. Figure 7 shows the predicted flux distribution for a circular coil supplied at 1250Hz lying on a copper slab. The corresponding normalized impedance values are given in Table 1.

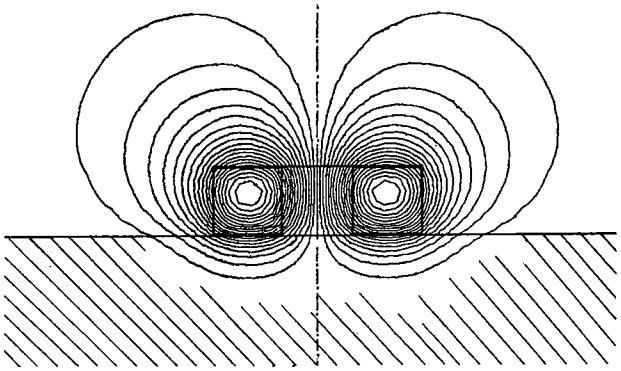

Fig. 7. Flux distribution for a coil on a copper slab at 1250Hz.

Case 3: - coil encircling a two conductor rod. Figure 8 shows the finite element predicted flux distribution for this case with the corresponding normalized impedance values given in Table 1 at

1250 Hz.

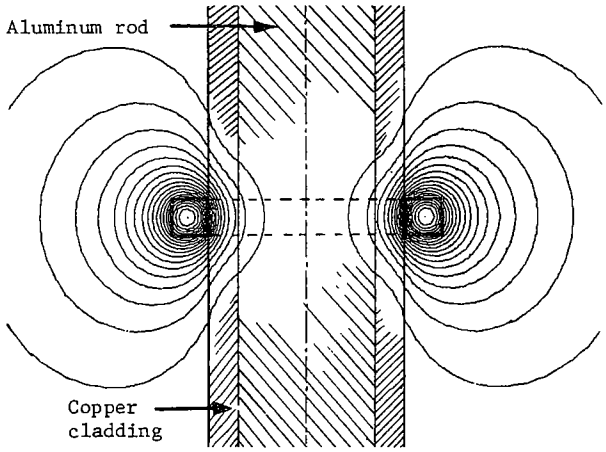

Fig. 8. Flux distribution for coil encircling a two-conductor rod.

Case 4: - coil centered over a flat-bottomed hole in a copper slab. Figures 9a) and b) show the finite element predictions of flux lines for excitation frequencies of 500 and 5,000Hz respectively, the depth of penetration effects are clearly visible.

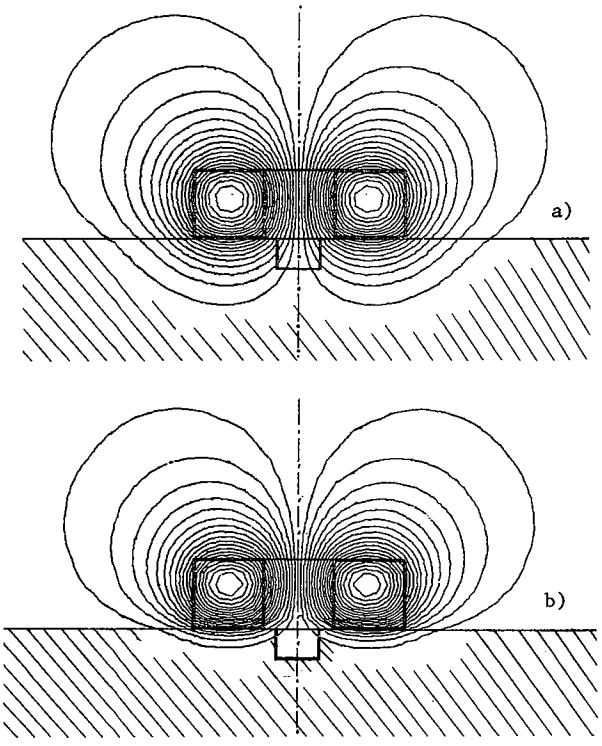

Fig. 9. Flux distribution at a) 500Hz and b) 5,000Hz for a coil lying on a copper slab with a flat bottomed hole.

Case 5: - coil inside a copper tube with an axisymmetric slot. Figures 10a) (copper tube) and b) iron tube) show the effect of tube permeability on the predicted flux distribution. Both plots are for an excitation frequency of 500Hz and the "shielding" effect of the higher permeability iron tube is clearly visible.

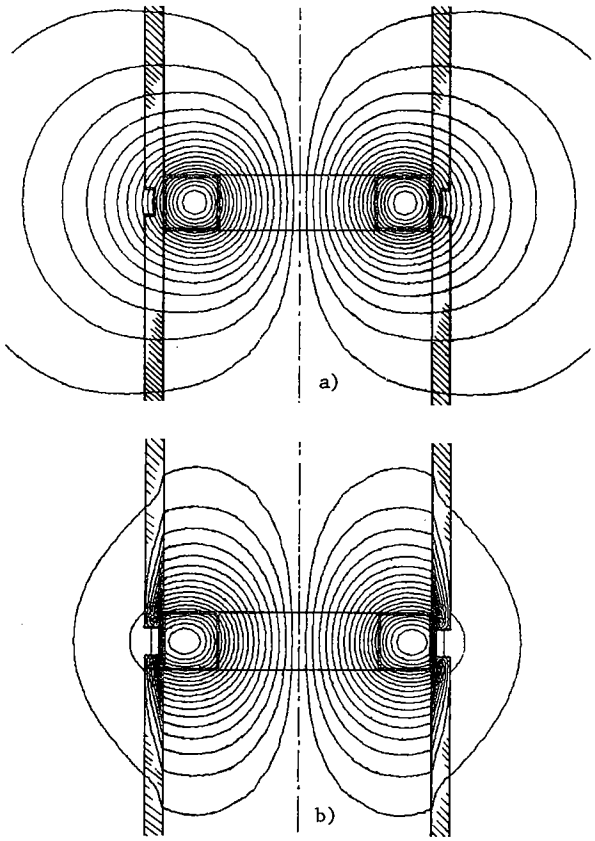

Fig. 10. Flux distribution around a coil in a) a copper tube and b) an iron tube at 500Hz.

Case 6: - coil encircling an iron rod. Figures 11a) and b) show the effect of an axisymmetric slot on the flux distribution in an iron rod encircled by a coil carrying current at 500Hz.

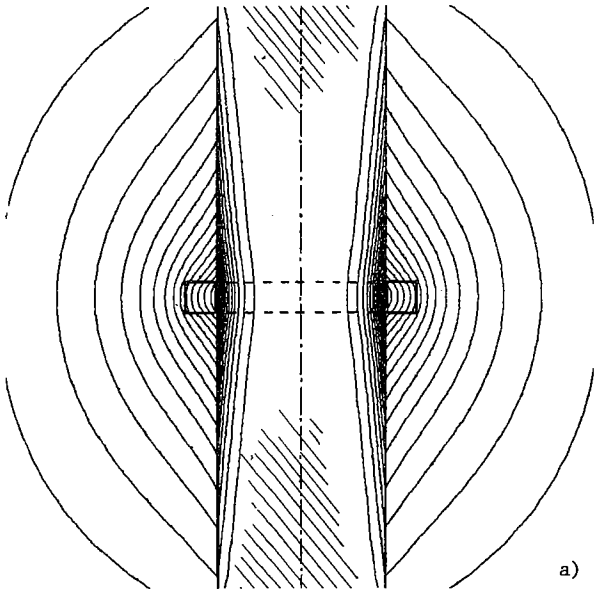

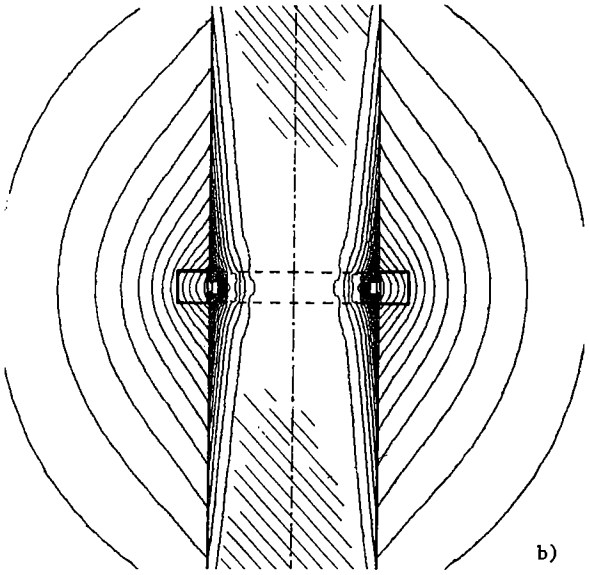

Fig. 11. Flux distribution around a coil encirling a) a plane iron rod and b) an iron rod with an axisymmetric defect.

DISCUSSION

Initial finite element studies of eddy current geometries appear promising. Where corresponding analytical and/or other numerical models exist, good agreement has been obtained with the finite element predictions. This observation is not surprising in that such methods have previously been used with success in the study of eddy current phenomena in electrical machinery. Indeed, if recent progress in the general area of finite element analysis is any yardstick, it should be reasonably safe to predict the solution of nonlinear, 3-dimensional, moving probe eddy current problems within the foreseeable future.

ACKNOWLEDGMENTS

This work is supported by the Electric Power Research Institute under contract RP1395-3 and the Army Research Office under grant DAAG29-76-G-0249.

REFERENCES

1. Bray, D. E. "Railroad Accidents and Nondestructive Inspection". Presented at the ASME Winter Annual Meeting, Paper No. 74-WA/RT-4, November 17, 1974.

2. Darcy, G. "Economic Motivation and Potential Impact of NDE in DOD, Proceedings of the Interdisciplinary Workshop for Quantitative Flaw Definition". AFML publication TR-73-238, June 1974, pp. 68-84.

3. Knight, S. R. "NDT for Nuclear Power". Materials Evaluation, May 1973, pp. 19-24.

4. Dau, G. J. "Rationale for Inservice Inspection During Nuclear Power Plant Design/Fabrication". Presented at the American Nuclear Society 23rd Annual Meeting, New York, June 1977.

5. Thompson, R. B. "Overview of the ARPA/AFML Program for Quantitative Flaw Definition". Proceedings of the ARPA/AFML Review of Progress in Quantitative NDE, AFML publication TR-77-44, September 1977, pp. 109-115. (Several papers relating to this work appeared in the first edition of the quarterly Research Supplement to Materials Evaluation, April 1977).

6. Adler, L. and Lewis, D. K. "Models for the Frequency Dependence of Ultrasonic Scattering from Real Flaws". ibid., pp. 180-186.

7. Krumhansl, J. A. "Interpretation of Ultrasonic Scattering Measurements by Various Flaws from Theoretical Studies". ibid., pp. 164-172.

8. Mucciardi, A. N. "Adaptive Nonlinear Modeling for Ultrasonic Signal Processing". Proceedings of the Interdisciplinary Workshop for Quantitative Flaw Definition. AFML publication TR-74-238, June 1974, pp. 194-212.

9. Stumm, W. "Multiparameter-Methoden in der Zerstorungsfreien Werkstoffprüfung". Materialprüfung. Vol. 19, April 1977, pp. 131-136.

10. Sukhorukov, V. V., Ullitin, Y. M., Chernov, L. A. "Feasibility of Determining Defect Parameters by Eddy Current Modulation Defectoscopy." Defektoskopiya. No. 1, January-February, 1977.

11. Brown, R. L., "Investigating the Computer Analysis of Eddy Current NDT Data", Hanford Engineering Development Laboratory Report, HEDL-SA-1721, February 1979.

12. Scott, I. G. "Eddy Current Problems in Nondestructive Testing", The Institution of Engineers, Australia Electrical Engineering Transactions, Vol. EE10, No. 1, 1974, pp. 46-53.

13. Lammeraner, J. and Stafl, M. "Eddy Currents", Iliffe Books, Ltd., 1966.

14. Stoll, R. L. "The Analysis of Eddy Currents", Clarendon Press, 1974.

15. Stoll, R. L. "Solution of Linear Steady State Eddy Current Problems by Complex Successive Overrelaxation", Proceedings IEE, Vol. 117, No. 7, July 1970, pp. 1317-1323.

16. Zhukov, V. K. and Zabirov, R. M. "Conductive Elliptical Cylinder in a Cross-sectionally Varying Uniform Magnetic Field", Defektoskopiya, No. 5, September-October 1970, pp. 102-109.

17. Schieber, D. "Transient Eddy Currents in Thin Metal Sheets", IEEE Transactions on Magnetics, Vol. MAG-8, No. 4, December 1972, pp. 775-779.

18. Carpenter, C. J. "A Network Approach to the Numerical Solution of Eddy Current Problems", IEEE Transactions on Magnetics, Vol. MAG-11, No. 5, September 1975, pp. 1517-1522.

19. Demirchian, K. S. et al, "Scalar Potential Concept for Calculating the Steady Magnetic Fields and Eddy Currents", IEEE Transactions on Magnetics, Vol. MAG-12, No. 6, November 1976, pp. 1045-1046.

20. Freeman, E. M. "Computer-aided Steady-state and Transient Solutions of Field Problems in Induction Devices", Proceedings IEE, Vol. 124, No. 11, November 1977, pp. 1057-1061.

21. McWhirter, J. H. et al, "A Computational Method for Solving Eddy Current Problems via Fredholm Integral Equations", submitted for publication in the IEEE Transactions on Magnetics.

22. Burrows, M. "Theory of Eddy Current Flaw Detection", Ph.D. Thesis, University of Michigan, 1964.

23. Dodd, C. V. "A Solution to Electromagnetic Induction Problems", M.S. Thesis, University of Tennessee, 1965.

24. Dodd, C. V. "Solutions to Electromagnetic Induction Problems", Ph.D. Thesis, University of Tennessee, 1967.

25. Dodd, C. V. et al, "Some Eddy Current Problems and their Integral Solutions", Oak Ridge National Laboratory, Contract No. W-7405-eng-26, April 1969.

26. Luquire, J. W. et al, "Computer Programs for some Eddy Current Problems", Oak Ridge National Laboratory, Contract No. W-7405-eng-26, August 1969.

27. Lord, W., Bridges, J. M., Yen, W., Palanisamy, R. "Residual and Active Leakage Fields Around Defects in Ferromagnetic Materials", Materials Evaluation 36, no. 8, (1978): 47.

28. Winslow, M. A. "Numerical Solution of the Quasilinear Poisson Equation in a Nonuniform Triangle Mesh". Journal of Computational Physics, Vol. 2, 1967, pp. 149-172.

29. Chari, M. V. K., and Silvester, P. "Finite Element Analysis of Magnetically Saturated dc Machines". IEEE Transactions on Power Appartus and Systems, Vol. 90, 1971, pp. 2362-2372.

30. Anderson, O. W. "Transformer Leakage Flux Program Based on the Finite Element Method". IEEE Transactions on Power Apparatus and Systems, Vol. 92, 1973, pp. 682-689.

31. Lord, W., and Hwang, J. H. "Finite Element Modeling of Magnetic Field/Defect Interactions". ASTM Journal of Testing and Evaluation, Vol. 3, No. 1, January 1975, pp. 21-25.

32. Hwang, J. H., and Lord, W. "Magnetic Leakage Field Signatures of Material Discontinuities". Proceedings of the Tenth Symposium on Nondestructive Evaluation, San Antonio, April 1975, pp. 63-76.

33. Lord, W., and Hwang, J. H. "Defect Characterization from Magnetic Leakage Fields", British Journal of Nondestructive Testing, Vol. 19, No. 1, January 1977, pp. 14-18.

34. Chari, M. V. K. "Finite Element Solution of the Eddy Current Problem in Magnetic Structures". IEEE Transactions on Power Appartus and Systems, Vol. 93, No. 1, January-February 1974.

35. Okuda, H. "Finite Element Solution of Traveling Wave Magnetic Field and Eddy Current". Electrical Engineering in Japan, Vol. 96, No. 4, 1976, pp. 75-82.

36. Sato, T., et al, "Calculation of Magnetic Field Taking into Account Eddy Current and Nonlinear Magnetism". Electrical Engineering in Japan, Vol. 96, No. 4, 1976, pp. 96-102.

37. Brauer, J. R. "Finite Element Analysis of Electromagnetic Induction in Transformers". Presented at the IEEE Winter Power Meeting, New York, January 1977.

38. Anderson, O. W. "Finite Element Solution of Skin Effect and Eddy Current Problems". Presented at the IEEE PES Summer Meeting, Mexico City, July 1977.

39. Csendes, Z. J. and Chari, M. V. K. "Finite Element Analysis of Eddy Current Effects in Rotating Electric Machines". Presented at the IEEE PES Summer Meeting, Mexico City, July 1977.

40. Chari, M. V. K., and Csendes, Z. J. "Finite Element Analysis of the Skin Effect in Current Carrying Conductors". IEEE Transactions on Magnetics, Vol. 13, No. 5, September 1977, pp. 1125-1127.

41. Demerdash, N. A. and Nehl, T. W. "Solution of Nonlinear Eddy Current and Loss Problems in the Solid Rotors of Large Turbogenerators using a Finite Element Approach". Presented at the PES Winter Meeting, January 1978.

42. Aldefeld, B. "Electromagnetic Field Diffusion in Ferromagnetic Materials". Proceedings IEE, Vol. 125, No. 4, April 1978, pp. 278-282.

43. Chari, M. V. K. and Kincaid, T. G., "The Application of Finite Element Method Analysis to Eddy Current NDE", ARPA/AFML Review of Progress in Quantitative NDE, July 1978.

44. Palanisamy, R. and Lord, W., "Theoretical Aspects of Eddy Current Testing", ASNT National Spring Conference Paper Summaries, April 1979, pp. 138-143.

45. Isaacson, E. and Keller, H. B., Analysis of Numerical Methods, John Wiley & Sons, Inc., New York, 1966.

46. Segerlind, L. J., Applied Finite Element Analysis, John Wiley & Sons, Inc., New York, 1976.